

Analysis of Poincaré plot derived from 5-min electrocardiography in dogs with myxomatous mitral valve disease

Radu Andrei Baisan, Cătălina Andreea Turcu, Eusebiu Ionuț Condurachi & Vasile Vulpe

To cite this article: Radu Andrei Baisan, Cătălina Andreea Turcu, Eusebiu Ionuț Condurachi & Vasile Vulpe (2023) Analysis of Poincaré plot derived from 5-min electrocardiography in dogs with myxomatous mitral valve disease, *Veterinary Quarterly*, 43:1, 1-10, DOI: [10.1080/01652176.2023.2212737](https://doi.org/10.1080/01652176.2023.2212737)

To link to this article: <https://doi.org/10.1080/01652176.2023.2212737>



© 2023 The Author(s). Published by Informa UK Limited, trading as Taylor & Francis Group.



[View supplementary material](#)



Published online: 24 May 2023.



[Submit your article to this journal](#)



Article views: 1278



[View related articles](#)



[View Crossmark data](#)

Analysis of Poincaré plot derived from 5-min electrocardiography in dogs with myxomatous mitral valve disease

Radu Andrei Baisan, Cătălina Andreea Turcu, Eusebiu Ionuț Condurachi and Vasile Vulpe

Clinic Department, Faculty of Veterinary Medicine, “Ion Ionescu de la Brad” Iasi University of Life Sciences, Romania

ABSTRACT

Background: Evaluation of heart rate variability (HRV) is used for risk assessment in a variety of cardiac diseases including myxomatous mitral valve degeneration (MMVD).

Objectives: To compare the geometric analysis of HRV using visual patterns of Poincaré plot among different classes of MMVD in dogs and to analyse the differences in beat-to-beat variability using tachograms and sequential Poincaré plots among different shapes.

Animals and methods: Healthy and MMVD dogs were retrospectively reviewed. Five-minute ECG data was used to create Poincaré plots and shapes were compared among groups. Furthermore, a sub-analysis of 50 consecutive R–R intervals was performed. Pearson Chi-square with adjusted standardized residuals was used to compare the categorical data between groups.

Results: Fifteen healthy dogs and 157 dogs with MMVD were included in the study. Normal and B1 groups showed a predominance of triangular shape (73% and 60% respectively; $p < 0.05$). In B2 group the predominant shape was comet (40%; $p < 0.05$) while comet and torpedo were predominant in Ca group (41% and 36% respectively; $p < 0.05$). Visual geometric analysis revealed a lower dispersion of the cloud clustering towards the left lower corner of the plot with MMVD progression. Diamond and triangle revealed a lower mean heart rate compared to comet and torpedo shapes ($p < 0.01$). Interclass correlation between 3 observers was 0.906 (95% CI of 0.8–0.96).

Conclusions: Poincaré plot shape changes with MMVD progression suggesting that geometrical analysis of HRV in dogs with cardiac conditions could be a useful tool in the risk assessment and further studies are warranted.

ARTICLE HISTORY

Received 26 September 2022

Accepted 5 May 2023

KEYWORDS

autonomic nervous system; heart rate variability; left atrium; Lorenz plot; R-R interval; sinus arrhythmia; sympathetic; parasympathetic


1. Introduction

Myxomatous mitral valve degeneration (MMVD) is the most common acquired cardiac disease in dogs, accounting for approximately 75% of heart disease cases and 10% of dogs presented to primary care veterinary practices (Keene et al. 2019). It had been shown that selected echocardiographic and radiographic variables can aid in the prediction of MMVD progression (Lord et al. 2011; Hezzell et al. 2012). However, development of predictive risk stratification schemes is of major interest for this disease (Keene et al. 2019). Heart rate variability (HRV) is a simple and non-invasive method and had been used for risk assessment in a variety of cardiac diseases for people and dogs (Malik et al. 1996; Kleiger et al. 2005; Oliveira et al. 2014; Bogucki and Noszczyk-Nowak 2017; Pirintra et al. 2017; Baisan et al. 2021). Sinus arrhythmia is a marker of health in both humans and dogs (Shaffer et al. 2014; Moise et al. 2019) and results from dynamic inputs of sympathetic and parasympathetic

systems modulated by complex mechanisms among which cardiovascular reflexes and mechanics of respiration are present (Moise et al. 2019).

In a previous study, we showed that HRV expressed through time and frequency domain is reduced with the disease progression (Baisan et al. 2021). More recently, several studies analyzed the normal beat-to-beat patterning and diagnostic value for detecting arrhythmias using geometrical analysis of Poincaré plot derived from one and 24-h Holter recordings in dogs (Blake et al. 2018; Moise et al. 2019; DeProspero and Adin 2020; Moise et al. 2021; Romito et al. 2021). To the authors' knowledge, there is no data regarding the geometrical analysis of HRV derived from 5-min electrocardiographic (ECG) recording in dogs with different classes of MMVD. Based on our observations, the geometrical distribution varies among dogs with different classes of MMVD. Therefore, we hypothesized that 5-min ECG derived Poincaré plot would vary with disease progression.

CONTACT Cătălina Andreea Turcu  catalina.andreea.turcu@gmail.com

 Supplemental data for this article can be accessed here <https://doi.org/10.1080/01652176.2023.2212737>.

© 2023 The Author(s). Published by Informa UK Limited, trading as Taylor & Francis Group.

This is an Open Access article distributed under the terms of the Creative Commons Attribution-NonCommercial License (<http://creativecommons.org/licenses/by-nc/4.0/>), which permits unrestricted non-commercial use, distribution, and reproduction in any medium, provided the original work is properly cited. The terms on which this article has been published allow the posting of the Accepted Manuscript in a repository by the author(s) or with their consent.

The aim of the study was to compare the geometric analysis of HRV using qualitative (visual patterns) of Poincaré plot among different classes of MMVD in dogs and to analyse the differences in beat-to-beat variability using tachograms and sequential Poincaré plots construction among the different shapes of Poincaré plots.

2. Animals and methods

This retrospective observational study included dogs presented for cardiologic examination at the Cardiology unit of the Veterinary Teaching Hospital, between January 2018 and July 2022. Ethical approval was obtained from the Ethics Committee of the Faculty of Veterinary Medicine of Iași (number 1051/2022, 1st of September, 2022). Electrocardiographic tracings of healthy dogs and dogs with a diagnosis of MMVD were reviewed. In MMVD group, dogs were included if the following data was available: echocardiography with changes consistent to MMVD, at least 5-min ECG recording in six standard leads, thoracic radiography and only those that did not receive any prior cardiovascular therapy. Dogs with pulmonary hypertension class 2B (Reinero et al. 2020) were accepted in the study. For dogs that required medication, therapy was assigned immediately after the cardiologic examination was finished. Any unstable dog that required therapy before a complete cardiologic examination was excluded from the study. Dogs with sustained arrhythmias or low quality tracing, dogs with congenital or acquired cardiac diseases other than MMVD and dogs with systemic diseases based on clinical examination were excluded. An age and body weight matched group of healthy dogs that were subjected to a complete cardiologic consultation for different reasons (e.g. prior to anesthesia for neutering) was included in the study as control.

All dogs were subjected to a complete cardiologic examination consisting of physical examination, followed by a five minutes six lead electrocardiography, echocardiography, and thoracic radiography. All dogs underwent the same examination order respecting an in-house protocol except the thoracic radiography which was performed before the ECG and echocardiography in dogs with clinical CHF. The diagnosis of MMVD was defined as echocardiographic evidence of mitral valve (MV) thickening and/or prolapse, with the presence of a regurgitating jet.

Furthermore, dogs were classified according to ACVIM recommendations (Keene et al. 2019) in class B1, dogs with a mitral valve regurgitation and absence of both left ventricle (LV) or left atrial (LA) enlargement and no clinical symptoms, class B2, dogs with enlargement of LV and LA in the absence of clinical signs and class Ca, defined as dogs with evidence of acute/concurrent pulmonary edema on radiography secondary to MMVD. Echocardiography was performed as previously described (Thomas et al. 1993) and assessed the morphology and

movement of the MV, the left ventricular internal diameter in diastole normalized to body-weight (LVIDd_n) as recently described using a scaling exponent of 0.33 (Rishniw and Brown 2022) with a cutoff of 1.7 (Boswood et al. 2016) and the LA/Ao ratio using a cutoff of 1.6 (Keene et al. 2019). Color and spectral Doppler were used to assess the presence of a regurgitating jet over the mitral and tricuspid valves, assessment of the transmitral flow pattern (E and A waves) and peak velocities of the pulmonary and aortic flows. Pulmonary hypertension was evaluated only based on the tricuspid regurgitation pressure gradient (TRPG) and was classified as mild (TRPG 36–50 mmHg), moderate (TRPG 51–75 mmHg) and severe (TRPG >75 mmHg) (Vezzosi et al. 2018; Feldhütter et al. 2022).

Electrocardiography was performed in the owner's presence, with a digital ECG machine (PolySpectrum 8E/8V, Neurosoft, Ivanovo, Russia) on dogs in right lateral or standing position with electrodes placed on the limbs, for at least 5 min at a speed of 50 mm/s and an amplitude of 10 mm/mV. The sampling rate used was 1000 Hz, with a 24-bit amplitude resolution. Electrocardiographic analyses were manually reviewed by a single operator (BRA) using a proprietary, dedicated software (PolySpectrum-Neurosoft v.4.8.118). Each ECG tracing was examined to ensure that the R–R intervals represented the P–P intervals. Throughout this manuscript the term R–R interval will be used as a surrogate for P–P interval as previously recommended (Moise et al. 2019). For further analysis of HRV, only sinus rhythm (SR) was used. Atrial or ventricular premature complexes, second degree atrio-ventricular blocks (AVB) and supraventricular runs were excluded along with the previous and subsequent sinus beat from the onset of the P-wave to the onset of the P-wave to ensure that the remaining R–R interval after the arrhythmia exclusion is not biased. The R–R intervals were then exported in an ASCII file and subjected to HRV analysis in a free dedicated software (Kubios HRV v.3.5.0, Kuopio, Finland). For visual assessment, each Poincaré plot was created from the raw R–R intervals expressed in milliseconds by plotting the data on separate columns (first column represented by R–R and second column represented by R–R+1) using GraphPad Prism (v. 5.03). Each dot represented an R–R interval (on X axis) plotted against and R–R+1 interval (on Y axis). Then the Poincaré plot was created for each dog by plotting the R–R data on X axis and R–R+1 data on Y axis and overlaid plot was created by stacking all Poincaré plots from all dogs in each group (normal and MMVD classes). The line of identity was defined as the major axis passing through the mean R–R interval along the bisector (Romito et al. 2021). Wave length was defined as the distance between adjacent crests of the R–R intervals tachogram waveform propagated in time. Sequential Poincaré plots were created for 10 consecutive R–R intervals to enable the visualisation of beat-to-beat patterning during short time periods and higher spatial resolution. The main cluster, represented by the

spatial distribution of the coordinates was visually analyzed and grouped according to the following shapes: diamond, represented by coordinates distribution on a square shape both along the line of identity and perpendicular to it; triangle represented by a triangular shape with the tip oriented towards the lower zone of the identity line and the base perpendicular to the identity line; comet shape represented by distribution of the coordinates along the identity line with a perpendicular narrow base towards the superior zone of the identity line; torpedo represented by coordinates clustered along the identity line with very narrow perpendicular distribution. If the cluster could not be included in any of the above patterns, it was characterized as undetermined shape. Subsequently, fifty R–R intervals of a representative ECG for each shape were analyzed using a parallel comparison between the HR and R–R tachogram with sequential construction of the Poincaré plot. Briefly, the raw R–R data from 5 min ECG tracing were uploaded in a free geometrical HRV analysis software (Flanders et al. 2022) and an epoch of 50 successive R–R intervals was selected. Then, the epoch was moved from the onset to the end of the 5 min period analyzing in real time the shape of the Poincaré plot. The most representative epoch of 50 R–R intervals was selected for further analysis. An inter-observer agreement analysis was performed between three observers for a total of 20 Poincaré plots, five from each group chosen using the Microsoft Excell ‘random’ function.

Statistical analysis was performed using SPSS v.17 software (IBM, Armonk, NY, USA). Poincaré plot graphics, HR and R–R tachograms were generated using GraphPad Prism v. 5.03 (GraphPad, San Diego, CA, USA) and Microsoft Office Excel 2016 (Microsoft Corporation, Redmond, WA, USA). Data was tested for normality using Saphiro–Wilk test. Normally distributed data are expressed as mean and standard deviation ($M \pm SD$) and skewed data are expressed as median and interquartile range (Q1–Q3). Categorical data of sex and reproductive status are expressed as total numbers and the Poincaré plot shape is expressed as percentage. An one-way ANOVA with Bonferroni post hoc test was used to assess normally distributed continuous variables while Kruskal–Wallis and pairwise comparison post hoc test was used to compare continuous variables for non-normally distributed data among the 4 groups. Further comparison analysis using Student’s

t test for continuous variables and Pearson Chi-square with Fisher’s exact for proportions between Maltese and non-Maltese dogs were performed. Pearson Chi-square with adjusted standardized residuals was used to compare the categorical data between groups. An interclass correlation (ICC) was used to assess inter-observer measurement agreement for Poincaré plot models by a two-way mixed effect model for absolute agreement. Agreement of the investigators was considered ‘poor’, ‘fair’, ‘moderate’, ‘substantial’, and ‘very good’ when values were in range 0–0.2, 0.21–0.4, 0.41–0.6, 0.61–0.8, and 0.81–1 (Barnhart et al. 2016). A *P* value <0.05 was considered statistically significant.

3. Results

One hundred seventy-two dogs met the inclusion criteria. The population comprised the following breeds: mix breed ($n=60$), Maltese ($n=53$), Poodle ($n=18$), Yorkshire terrier ($n=9$), Shih–Tzu ($n=7$), Chihuahua and Beagle ($n=6$ of each), Pinscher ($n=5$), Daschund ($n=4$), and one of each Pekingese, Cavalier King Charles Spaniel, French bulldog and Spitz. In three dogs the reproductive status was unknown. The demographic and clinical data for the entire population and each group are presented in Table 1. There was no significant difference between age and body weight between groups. Furthermore, no statistical difference for clinical and echocardiographic variables between non-Maltese and Maltese dogs was observed, except BW which was lower in the latter group ($p<0.01$).

Supraventricular premature complexes were detected and removed in 41 dogs, ventricular premature complexes in 14 dogs, 2nd degree AVB in 2 dogs and supraventricular runs in 1 dog. None of the dogs from healthy group had any arrhythmias. The number of dogs with arrhythmias for each class and the mean and range of each arrhythmias excluded are presented in Supplementary file 1. Echocardiographic data are presented in Table 2. Fifteen healthy dogs were included in N group. Based on ACVIM classification of MMVD (Keene et al. 2019), 76 dogs were diagnosed as class B1, 37 dogs as B2 and 44 dogs as class Ca. All dogs in class Ca had evidence of pulmonary edema on radiography and none of the dogs in classes B1 or B2. There was no statistically significant difference in proportions of Maltese dogs among groups of dogs based on

Table 1. Dog demographic and clinical data on the entire population and divided into normal group and groups according to ACVIM classification for myxomatous mitral valve disease.

Variable	Total ($n=172$)	<i>N</i> ($n=15$)	B1 ($n=76$)	B2 ($n=37$)	Ca ($n=44$)
Age	12 (9–13)	10.2 (6.5–13.2)	12 (9.2–13)	11 (9–14)	11 (8.8–14)
Body weight	6.4 (5–8.4)	5.8 (4.6–8.1)	7 (5.2–9)	6 (5.4–8.7)	6.2 (4.7–8.1)
Sex (M/F)	107/65	9/6	43/33	26/11	29/15
Neuter status (Y/N)	52/117	7/8	22/52	9/27	14/30
Respiratory rate	44 ± 21	29 ± 3.4	34 ± 13	39 ± 10	64 ± 23**
Heart rate	135 ± 28	115 ± 22	120 ± 21	142 ± 25*	160 ± 21**

M, male; F, female.

*Statistical difference between classes B1 and B2

**Statistical difference between classes B2 and Ca

Table 2. Echocardiographic measurements of dogs diagnosed with MMVD divided by ACVIM classification.

Variable	N (n=15)	B1 (n=76)	B2 (n=37)	Ca (n=44)
LA/Ao	1.32±0.1	1.41±0.19	2.04±0.35*	2.13±0.34
LVIDd_n	1.22±0.17	1.39±0.17	1.86±0.21*	1.82±0.31
E wave velocity (m/s)	0.67±0.25	0.7±0.16	1.14±0.22*	1.28±0.33
TR PG (mmHg)	–	43.7±5.4	44.7±7.1	48.9±12

La/Ao, left atrial to aorta ratio; LVIDd_n, left ventricular internal diameter in diastole normalized to body-weight using an exponent of 0.33; TR PG, tricuspid regurgitation pressure gradient.

*Statistical difference between classes B1 and B2

Table 3. Poincaré plot shapes percentage in different groups of healthy and MMVD dogs.

Groups	Diamond (%)	Triangle (%)	Comet (%)	Torpedo (%)
N (n=15)	20	73.3	6.7	0
B1 (n=68)	11.8	60.3	14.7	13.2
B2 (n=35)	5.7	28.6	40	25.7
Ca (n=39)	0	23.1	41	35.9

Dogs with undetermined shape on Poincaré were excluded from this table.

diagnosis. Thirty-two dogs had pulmonary hypertension (PH): four dogs in class B1, seven dogs in class B2 and 21 dogs in class Ca. Dogs in classes B1 and B2 had only mild PH. In class Ca, 14 dogs had mild, 6 dogs had moderate and one dog had severe PH.

Visual analysis of the Poincaré plot derived from each ECG tracing was assessed and grouped as diamond, triangle, comet and torpedo shape. Undetermined shape was detected in 15 dogs (8 in B1, 2 in B2 and 5 in Ca groups). Dogs with undetermined shape were excluded from further analysis. A statistically significant association between groups of dogs and Poincaré plot shape was observed ($p < 0.01$). Normal and B1 groups showed a predominance of triangular shape (73% and 60% respectively; $p < 0.05$). In B2 group the predominant shape was comet (40%; $p < 0.05$) while for group Ca the predominant shapes were comet and torpedo (41% and 36% respectively; $p < 0.05$). The percentage of different Poincaré plot shapes in different groups of dogs is presented in Table 3. There was no statistically significant difference in the proportion of Poincaré plot shapes between Maltese and non-Maltese dogs on the entire population nor when groups were divided by ACVIM class.

Furthermore, there was a statistically significant difference in HR between diamond and comet ($p < 0.01$), diamond and torpedo ($p < 0.01$), triangle and comet ($p < 0.01$) and triangle and torpedo ($p < 0.01$), where diamond and triangle groups showed a lower mean heart rate compared to comet and torpedo. Patterns of Poincaré plot detected in the study population are presented in Figure 1.

When Poincaré plot graphics were overlapped by groups, healthy dogs revealed a triangular shape while dogs in B1 showed a triangular shape with larger distribution over X and Y axis demonstrating a variation of short-long (left upper area), long-short (right lower area), long-long (right upper area) and short-short R-R intervals (left lower area). In class B2, the Poincaré plot overlapping revealed a narrower distribution perpendicular to the line of identity. This is explained by a lower amount of long-short and short-long intervals as compared to

B1 dogs. Also, there is a lower density of points in the upper right area demonstrating a lower number of long-long cycles and the cloud shifts towards the left lower area. In class Ca, the density of points is displayed in the lower left area demonstrating that the beat-to-beat patterning in these dogs is overrepresented by short-short intervals. Visual geometric analysis revealed that with MMVD progression, the dispersion of data points reduces and the cluster is moving towards the left lower corner of the plot demonstrating a denser region of short-short intervals (Figure 2).

Subsequently, a subanalysis for each type of Poincaré plot performed from a 50R-R intervals sample was carried out. Electrocardiographic tracings with a diamond shape Poincaré plot revealed large beat-to-beat variation on HR tachogram as seen in Figure 3A where the bars, representing the instantaneous HR, show different heights with a non-linear variation. On R-R tachogram (Figure 3B) there is a large difference between high peaks (low instantaneous HR) and low peaks (high instantaneous HR) with a short wave length, (few coordinates on an ascending or a descending branch) indicating an abrupt and ample change in HR from one beat-to-beat interval to the following one. Furthermore, the sequential construction of the Poincaré plot (Figure 3C, boxes 1–5) represents the dynamic patterning of the beat-to-beat interval distribution for each 10 consecutive R-R intervals. Notably, larger variations with short wave length on R-R tachogram (e.g. Figure 3B, box 1) have a tendency of larger dots distribution in a triangular or rectangular shape (e.g. Figure 3C, box 1), while a smaller variation (e.g. Figure 3B, box 4) have a tendency of closer clustering (e.g. Figure 3C, box 5). Figure 3D presents the fully constructed Poincaré plot of 50R-R intervals selected for analysis.

Triangular shape Poincaré plot shows different beat-to-beat patterning. On HR tachogram the variation of successive instantaneous HR is smaller compared to diamond shape, however, this variation maintains a non-linear pattern. As shown in Figure 4A, a repetitive sequence of high-low (e.g. bars no. 17 and 18) and low-high (e.g. bars no. 18 and 19)

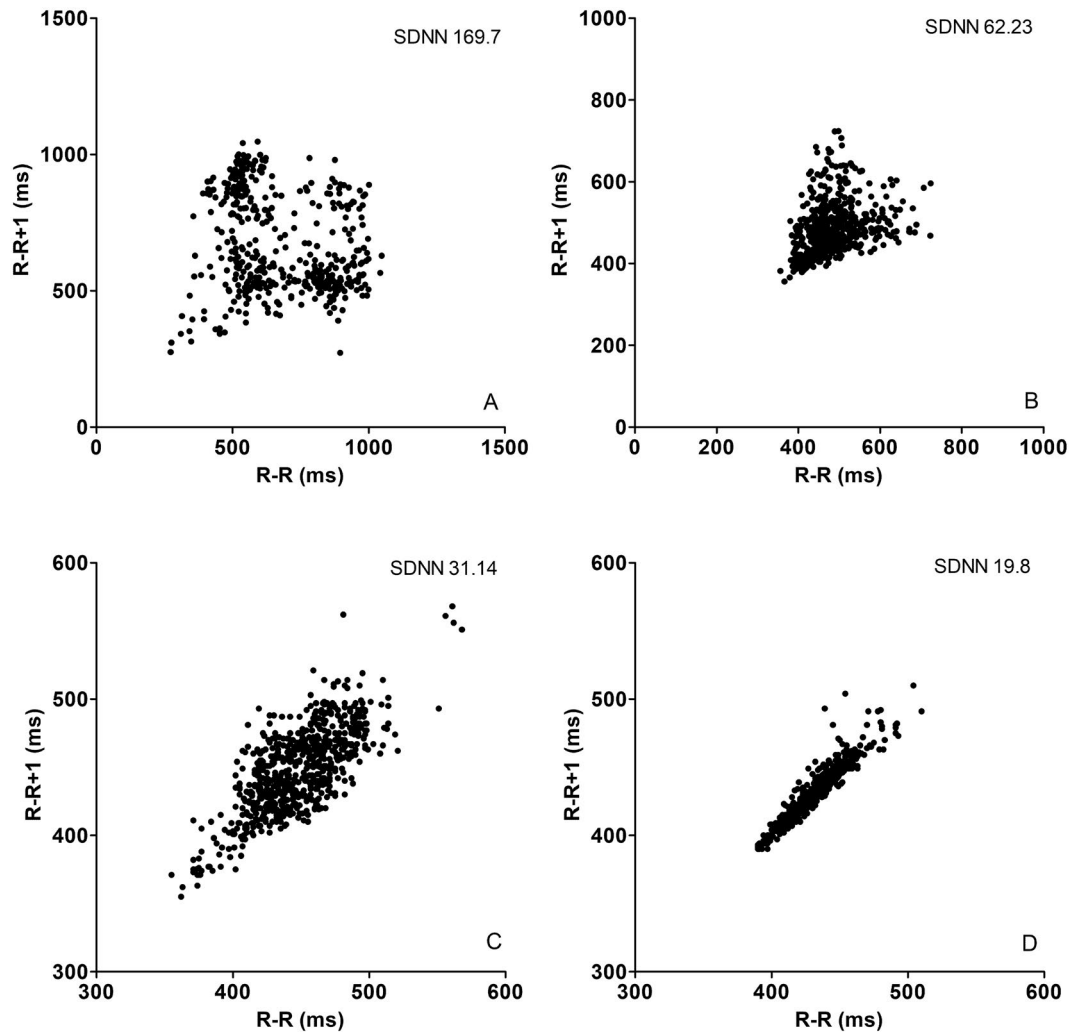


Figure 1. Representative Poincaré plot shapes derived from 5-min ECG recording with SDNN value (ms) for each tracing. Each point represents the coordinates in milliseconds for R-R (X axis) and R-R+1 (Y axis); A. diamond shape; B. triangle shape; C. comet shape; D. torpedo shape; SDNN—standard deviation of the NN intervals expressed in milliseconds.

is present. The R-R tachogram (Figure 4B) reveals predominantly low amplitude peaks alternating with higher amplitude peaks with short wave length (e.g. coordinates 17, 18 and 19 with no points on the ascending or descending branches). The sequential construction of the Poincaré plot reveals close clustering of the dots during periods of low variation (Figure 4B and C, box 4) consistent with the tip and body of the triangle (approximately similar length of R-R and R-R+1) and larger distribution of the dots with a triangular shape (Figure 4B and C, box 2) consistent with the edges of the triangle (sequences of long-short and short-long intervals). Figure 4D presents the completely constructed Poincaré plot of 50 R-R intervals selected for analysis.

The HR tachogram of the comet shape revealed a small linear variation in instantaneous HR with progressive increase and decrease in heart rate over short periods (Figure 5A). R-R tachogram shows small amplitude waves with longer wave length (multiple points on ascending and descending branches) (Figure 5B). The sequential Poincaré plot reveals a circular pattern with dots clustered in the lower part

of the identity line during higher heart rates (Figure 5C boxes 1–3) and slightly greater distribution with dots clustered in the upper part of the identity line during periods of lower HR (Figure 5C, boxes 3 and 4). Figure 5D presents the completely constructed Poincaré plot of 50 R-R intervals selected for analysis revealing a comet shape.

The HR tachogram of torpedo shape Poincaré plot revealed very small variations in HR (Figure 6A). R-R tachogram showed minimal amplitude waves with long wavelength and absence of any regular patterning. Sequential Poincaré plot showed closely clustered points traveling along the line of identity with minimum perpendicular dispersion (e.g. Figure 6C, box 2 and 3). Figure 6D presents the complete construction of the Poincaré plot from 50 R-R intervals with magnification due to the marked clustering of the points and small spatial resolution.

Poincaré plot shapes were reviewed by three different observers. Inter-observer agreement between all 3 observers, performed for 20 randomly selected Poincaré plots from all groups was very high, with an ICC of 0.906 (95% CI of 0.8–0.96).

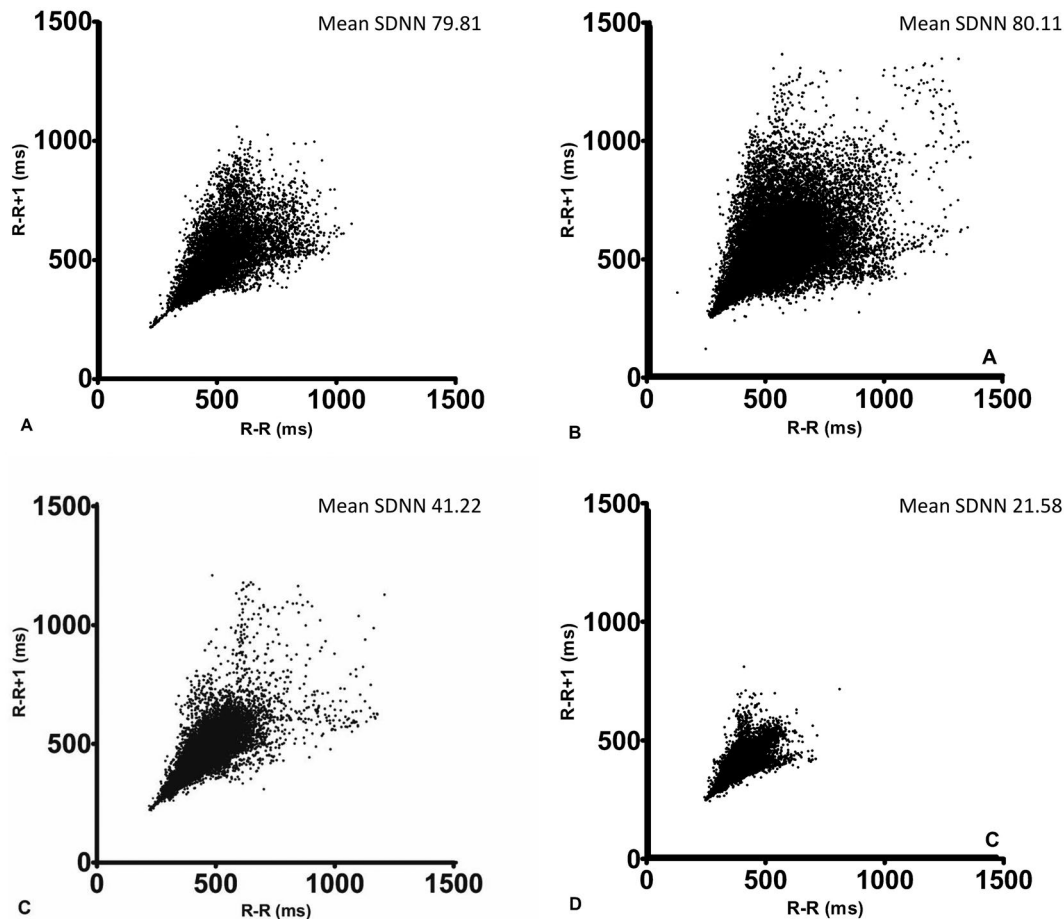


Figure 2. Overlapped Poincaré plots from normal dogs and dogs divided by ACVIM classes of severity with mean group value of SDNN (ms): A healthy dogs; B dogs in class B1; C dogs in B2; D dogs in class Ca; the X and Y axis scales are identical among graphics to underline the dynamics of point distribution between healthy dogs and dogs in different severity classes of MMVD; SDNN—standard deviation of the NN intervals expressed in milliseconds.

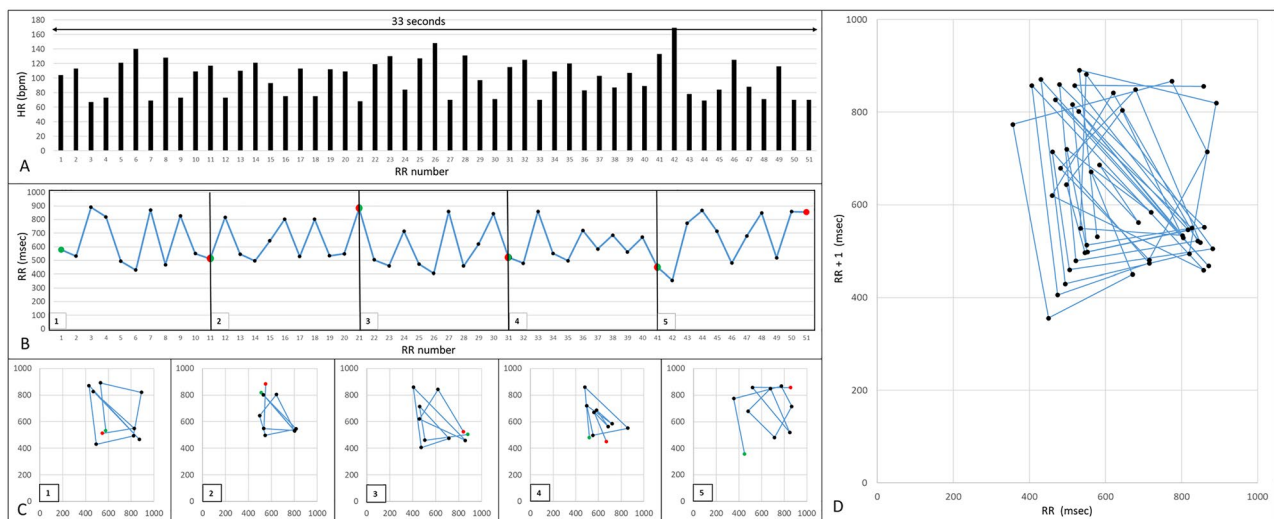


Figure 3. A. Heart rate tachogram, B. R-R tachogram and C, D. Poincaré plot construction from 50 R-R intervals in a dog with MMVD in class B1, with a mean HR of 101 bpm. Heart rate tachogram shows very large, nonlinear variations in heart rate characterized mainly by long-short and short-long pairs and occasionally short-short and long-long pairs. R-R tachogram reveals high amplitude spikes with very few coordinates on the ascending and descending branches explained by the nonlinear behavior of this pattern and the large variations between intervals. Sequences of Poincaré plots reveal a highly spread distribution across the identity line and perpendicular to it. The shapes representative for this pattern are triangles (sequences of short-short + short-long + long-short or long-short + short-short + long-short) or squares (sequences of short-short + short-long + long-long + long-short). Image D represents the final construction of the Lorenz plot derived from 50 R-R showing a 'diamond' shape.

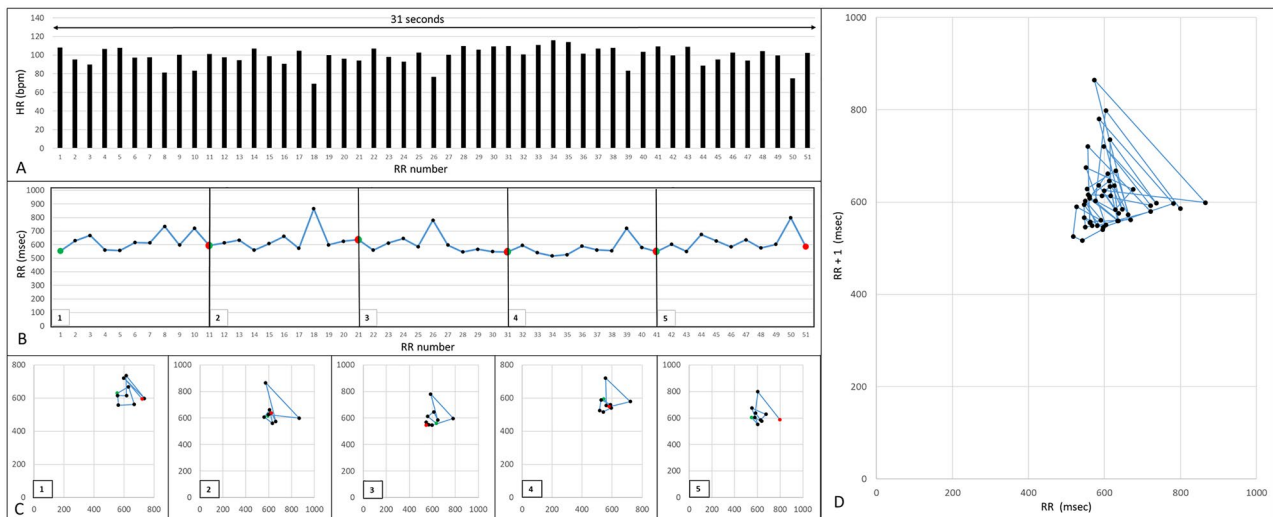


Figure 4. A. Heart rate tachogram, B. R–R tachogram and C, D. Poincaré plot construction from 50R–R intervals in a dog with MMVD in class B1 with a HR of 99 bpm. Heart rate tachogram shows short nonlinear fluctuations in heart rate comprising isolated larger variations. R–R tachogram (B) reveals alternations between small variations (e.g. R–R 4–7), medium variations (e.g. R–R 7–11) and large variations (e.g. R–R 17–19). Sequential Poincaré plots reveal alternations between periods with clustered dots (consistent with small variations in R–R intervals) and dispersed dots (consistent with larger variations in R–R intervals, e.g. box 4). D The construction of the Lorenz plot graphic revealing a triangle shape.

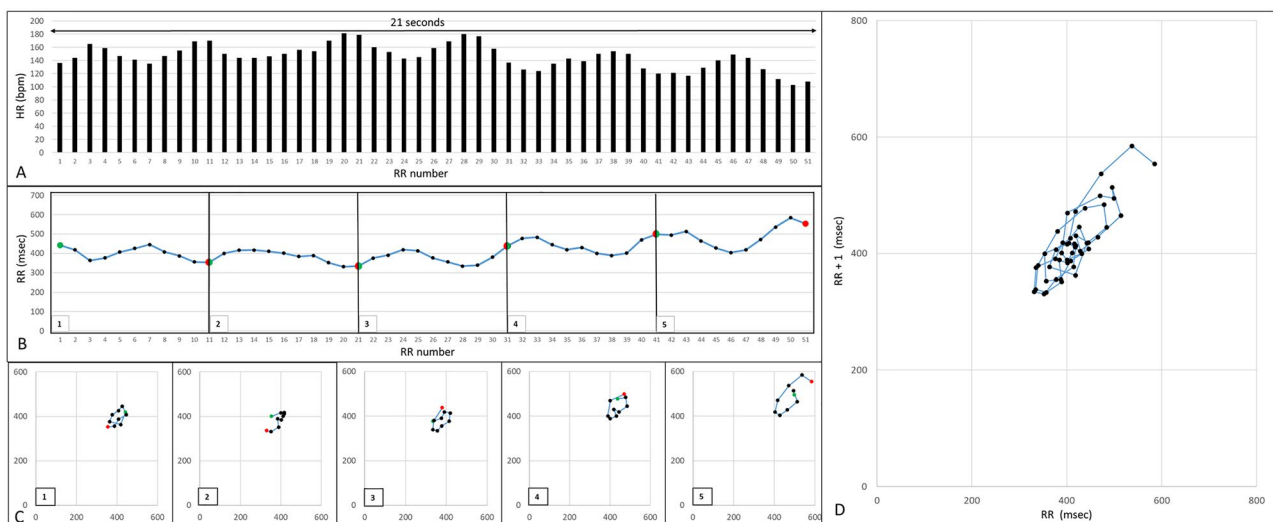


Figure 5. A. Heart rate tachogram, B. R–R tachogram and C, D. Poincaré plot construction from 50R–R intervals in a dog with MMVD in class B2 and a mean HR of 145 bpm. The HR tachogram shows rapid and linear fluctuations in HR and consecutive increase and decrease in rate, also represented in R–R tachogram. In sequential Poincaré plots 1–3 the R–R coordinates' distribution is smaller and the construction reveal a circular distribution. During the last two plots (4 and 5), associated with a mild decrease in HR on tachogram the R–R coordinates reveal a larger distribution with the same circular pattern. D The final construction of the Poincaré plot derived from a 50R–R intervals sequence revealing a 'comet' shape.

4. Discussion

Previous studies suggest that HRV is a useful method to evaluate cardiac autonomic modulation in humans and animals, as well as for risk assessment in a variety of cardiac diseases (Malik et al. 1996; Kleiger et al. 2005; Ootaki et al. 2008; Zhou et al. 2009; Rasmussen et al. 2011; Oliveira et al. 2014; Bogucki and Noszczyk-Nowak 2017). In a previous study, we found that HRV expressed by time and frequency domain decreases with the increase in MMVD severity (Baisan et al. 2021).

In the present study we aimed to evaluate the geometrical beat-to-beat variability through Poincaré plot analysis derived from a five-minute long electrocardiogram in healthy dogs and dogs diagnosed with different MMVD classes. In this study, for the assessment of geometrical beat-to-beat variability we only used sinus beats to ensure the true autonomic nervous system (ANS) behaviour, therefore any non-sinus arrhythmias were excluded. Moreover, we only included dogs at first presentation and before any cardiovascular therapy was administered,

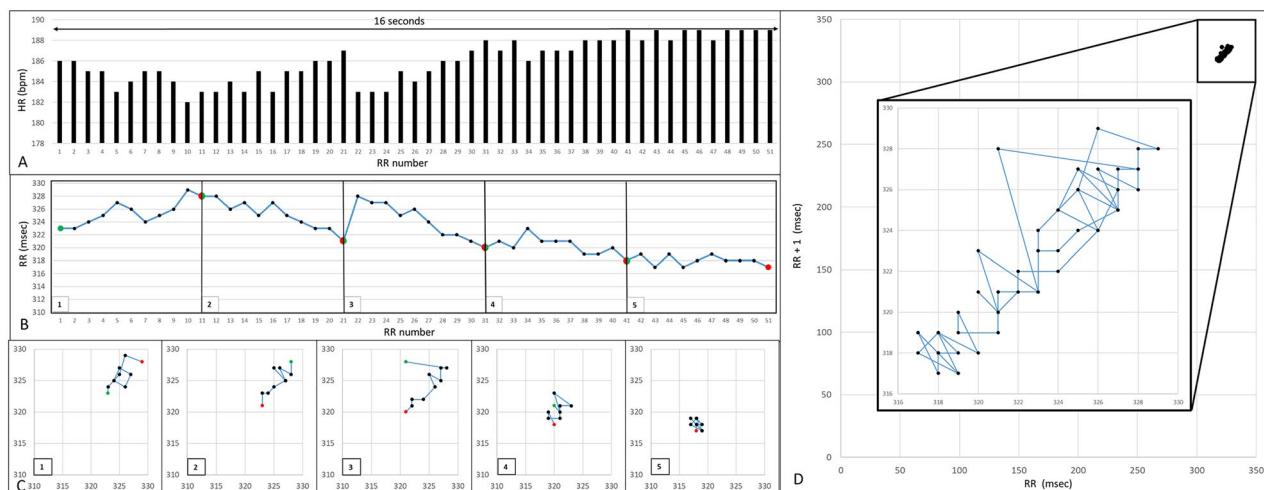


Figure 6. A. Heart rate tachogram, B. R–R tachogram and C, D. Poincaré plot construction from 50 R–R intervals in a dog with MMVD in class Ca with a mean HR of 186 bpm. The HR tachogram reveals short both linear and nonlinear changes in heart rate as well as periods with unremarkable variation (e.g. last part of the R–R tachogram, box 5). The R–R tachogram reveals very small variations in HR (between 0 and 2%) with no repetitive pattern. Note that the minimum variation in HR corresponding to the last part of the tachogram reveals a highly clustered distribution (B and C, box 5). D The final construction of the Lorenz plot derived from 50 R–R intervals—large graphic represents the distribution scaled to 350 ms and the small graphic represents the magnified distribution scaled to 14 ms highlighting the degree of variation in heart rate for this dog.

to avoid the potential effect of cardiac drugs on the dynamics of ANS.

Based on the visual analysis of the geometric patterning and according to the literature, the Poincaré plot shapes were classified in five groups as diamond, triangle, comet, torpedo and undetermined shape (Esperer et al. 2008; Moise et al. 2019; Romito et al. 2021). According to this assessment, we found an association between beat-to-beat clustering shape and disease severity. While healthy dogs and dogs with MMVD class B1 were associated mainly with diamond and triangle shapes, classes B2 and Ca were commonly associated with comet and torpedo shapes, respectively. In a previous study analyzing Poincaré plots from Holter recording in dogs, comet, and diamond shapes were associated with SR and normal HRV while torpedo shape was associated with SR and reduced HRV (Romito et al. 2021). In the present study we did not intend to compare HRV time or frequency domain results with Poincaré plot shape, however plots from dogs in more advanced MMVD classes (e.g. classes B2 and Ca) were associated with a narrower distribution of the cloud. Several studies have shown that a fan shape is exclusively associated with atrial fibrillation (DeProspero and Adin 2020; Romito et al. 2021). In our study, we used the term ‘triangle’ to avoid confusion with atrial fibrillation pattern since all of our dogs were in SR. However, some of our dogs exhibited a similar pattern on a 5-min recording because this shape was most probably corresponding to the ‘tip’ of the normal ‘Y’ shape on 24-h Holter recording. This may be explained by the fact that in the clinical setting, our patients did not reach the ‘branching’ point of the Poincaré plot, also called avoidance zone which emerges at a HR of 98–103 bpm also

being recorded during sleep hours (Moise et al. 2010; Moise et al. 2019). As expected, the mean HR showed differences between Poincaré plot shapes. Diamond and triangle shapes had significantly lower mean HR compared to comet and torpedo. This means that with heart rate increase, the coordinates distribution along and perpendicular to the line of identity decreases. Heart rate is controlled by ANS system and the balance between sympathetic and parasympathetic arms (Malik et al. 1996; Moise et al. 2019). However, there are other mechanisms associated with changes in HRV such as the regulatory mechanisms *via* respiratory sinus arrhythmia, the baroreceptor reflex and rhythmic changes in vascular tone (Shaffer and Ginsberg 2017). Respiratory sinus arrhythmia was shown to decrease with the increase in HR therefore, when SRA is such elevated as in the dog, HR and interbeat interval variability are also influenced by the breathing pattern (Grosso et al. 2021). In our study, respiratory rate was only significantly higher in dogs with MMVD class Ca. However, there was a trend of increase in rate even before acute CHF, a finding that is also supported by previous studies (Boswood et al. 2020). Moreover, we did not perform specific analysis on SRA because this requires dual channel parallel recording of ECG and respiratory curve (Grosso et al. 2021).

When all Poincaré plots from healthy dogs and dogs in class B1 were overlapped, the resulting graphic revealed a wide distribution both along the identity line and perpendicular to it. Dogs in MMVD class B2 revealed comet as the most common Poincaré plots shape. Comet shape is characterized by points placed along the line of identity (length larger than width), with only one central cluster revealing a smaller dispersion perpendicular to the

identity line (Romito et al. 2021). These findings may support the idea that ANS balance and beat-to-beat variability are altered in dogs with MMVD even before CHF is clinically visible. When Poincaré plots from dogs in class Ca were overlapped, the points clustered in the left lower area of the Poincaré plot corresponding to a high prevalence of short-short R-R intervals. This could be explained by the increase in the heart rate in dogs with congestive heart failure due to MMVD (Boswood et al. 2020; Baisan et al. 2021) and loss of sinus respiratory arrhythmia (López-Alvarez et al. 2015).

Subsequently, further parallel analysis on different patterns of Poincaré plots constructed from a period of 50 consecutive R-R intervals was attempted. This analysis permitted a step-by-step comparison between changes in HR and R-R tachogram and sequential (10 R-R intervals) Poincaré plots. In a diamond distribution, there was a high nonlinear variability among consecutive R-R intervals which was specific to lower heart rates. This behaviour had been shown in several studies and was associated with healthy dogs with normal SRA (Moise et al. 2019). Moreover, a previous research found that besides SRA, altered conduction and exit blocks in the sinoatrial conduction pathways may contribute to the behaviour of beat-to-beat variability in dogs (Moise et al. 2021). Similarly, at lower HR, beat-to-beat coordinates clustered in a triangular shape which was mostly found in healthy dogs and dogs in class B1. In these dogs, interbeat interval variation was smaller, however long-short and short-long sequences were present. As a difference to diamond shape these dogs did not have consecutive long-long intervals (which would cluster in the upper region of the identity line). This could be explained as long-long intervals are expected to have a higher prevalence during sleep (Moise et al. 2019) and high vagal tone bursts while the recording in our dogs was performed during awake period in the clinical environment. Comet shape was associated with higher heart rate. Interestingly, in this particular case, the beat-to-beat variability revealed a linear pattern with progressive increase and decrease in heart rate similar to human R-R variability (Moise et al. 2019). While in healthy human beings this behaviour appears at lower heart rates, this pattern was found mainly in dogs with cardiomegaly with and without evidence of pulmonary edema. Interestingly, in a previous study on dogs subjected to Holter monitoring, comet shape was associated with sinus respiratory arrhythmia and normal HRV (Romito et al. 2021) while in another study all healthy dogs presented a 'Y' shape (Blake et al. 2018). However, our analysis performed Poincaré plots derived from 5 min recording cannot be compared to 24-h Holter recordings. The torpedo shape was also encountered during faster heart rates and revealed both linear and nonlinear minimal changes in beat-to-beat variability resulting in a thin cluster along the line of identity, associated mostly with dogs in acute CHF due to MMVD. In a previous study we found a significant decrease in HRV time and frequency domain parameters once pulmonary

edema was clinically relevant (Baisan et al. 2021), therefore a low dispersion of the cluster is expected.

This study has several limitations. Five-minute electrocardiographic recording in the clinical environment may be altered by a variety of stimuli and HR or beat-to-beat intervals may behave differently from one dog to another which could bias our data. However, clinical environment includes all these stimuli and removing any interferences with ANS would result in a purely experimental study which was not our aim. Also, this study is mainly based on visual analysis and quantification of patterns is difficult and no gold standard is available for these methods. The description of Poincaré plots in this study could be shallow therefore we hope that these findings will promote further investigations in this field and further studies will shed light in the unique beat-to-beat patterning in dogs with different pathological conditions. Finally, our findings show individual variations as the same Poincaré plot shape can be found in different groups and these data should be interpreted in a clinical setting.

This study's findings indicate that Poincaré plot shapes tend to change with the MMVD severity. These results may be considered in risk assessment along with other biomarkers for dogs with MMVD especially since easy-to-use software for geometrical analysis of HRV are already available (Flanders et al. 2022). However, a widely accepted classification of the Poincaré plot shape is not yet available and future studies are needed for exploring the association between different biomarkers and beat-to-beat distribution during this pathological condition.

Conclusions

Our study demonstrated that Poincaré plot shape derived from 5 min ECG recording changes with MMVD progression where healthy dogs and dogs in class B1 have shown a higher prevalence of diamond and triangle shape while dogs in class B2 were associated with comet and those in class Ca with comet and torpedo shapes. Moreover, a focused analysis of beat-to-beat patterning comparing tachograms and sequential Poincaré plots revealed differences of the inter-beat intervals behaviour between different shapes. These findings suggest that geometrical analysis of HRV in dogs with cardiac conditions could be a useful tool in the risk assessment and further studies are warranted.

Funding details

This research received no external funding.

Disclosure statement

The authors report there are no competing interests to declare.

References

- Baisan RA, Vulpe V, Ohad DG. 2021. Short-term heart rate variability in healthy dogs and dogs in various stages of degenerative mitral valve disease evaluated before pharmacotherapy. *Vet J.* 274:105704.
- Barnhart HX, Yow E, Crowley AL, Daubert MA, Rabineau D, Bigelow R, Pencina M, Douglas PS. 2016. Choice of agreement indices for assessing and improving measurement reproducibility in a core laboratory setting. *Stat Methods Med Res.* 25(6):2939–2958.
- Blake RR, Shaw DJ, Culshaw GJ, Martinez-Pereira Y. 2018. Poincaré plots as a measure of heart rate variability in healthy dogs. *J Vet Cardiol.* 20(1):20–32.
- Bogucki S, Noszczyk-Nowak A. 2017. Short-term heart rate variability in dogs with sick sinus syndrome or chronic mitral valve disease as compared to healthy controls. *Pol J Vet Sci.* 20(1):167–172.
- Boswood A, Gordon SG, Häggström J, Vanselow M, Wess G, Stepien RL, Oyama MA, Keene BW, Bonagura J, MacDonald KA, et al. 2020. Temporal changes in clinical and radiographic variables in dogs with preclinical myxomatous mitral valve disease: the EPIC study. *Vet Intl Med.* 34(3):1108–1118.
- Boswood A, Häggström J, Gordon SG, Wess G, Stepien RL, Oyama MA, Keene BW, Bonagura J, MacDonald KA, Patteson M, et al. 2016. Effect of pimobendan in dogs with preclinical myxomatous mitral valve disease and cardiomegaly: the EPIC study: a randomized clinical trial. *J Vet Intern Med.* 30(6):1765–1779.
- DeProspero DJ, Adin DB. 2020. Visual representations of canine cardiac arrhythmias with Lorenz (Poincaré) plots. *Am J Vet Res.* 81(9):720–731.
- Esperer HD, Esperer C, Cohen RJ. 2008. Cardiac arrhythmias imprint specific signatures on Lorenz plots. *Ann Noninvasive Electrocardiol.* 13(1):44–60.
- Feldhütter EK, Domenech O, Vezzosi T, Tognetti R, Eberhard J, Friederich J, Wess G. 2022. Right ventricular size and function evaluated by various echocardiographic indices in dogs with pulmonary hypertension. *J Vet Intern Med.* 36(6):1882–1891.
- Flanders WH, Moise NS, Pariaut R, Sargent J. 2022. The next heartbeat: Creating dynamic and histographic Poincaré plots for the assessment of cardiac rhythms. *J Vet Cardiol.* 42:1–13.
- Grosso G, Vezzosi T, Briganti A, Di Franco C, Tognetti R, Mortola JP. 2021. Breath-by-breath analysis of respiratory sinus arrhythmia in dogs. *Respir Physiol Neurobiol.* 294:103776.
- Hezzell MJ, Boswood A, Moonarmart W, Elliott J. 2012. Selected echocardiographic variables change more rapidly in dogs that die from myxomatous mitral valve disease. *J Vet Cardiol.* 14(1):269–279.
- Keene BW, Atkins CE, Bonagura JD, Fox PR, Häggström J, Fuentes VL, Oyama MA, Rush JE, Stepien R, Uechi M, et al. 2019. ACVIM consensus guidelines for the diagnosis and treatment of myxomatous mitral valve disease in dogs. *J Vet Intern Med.* 33(3):1127–1140.
- Kleiger RE, Stein PK, Bigger JT, Jr. 2005. Heart rate variability: measurement and clinical utility. *Ann Noninvasive Electrocardiol.* 10(1):88–101.
- López-Alvarez J, Elliott J, Pfeiffer D, Chang Y-M, Mattin M, Moonarmart W, Hezzell MJ, Boswood A. 2015. Clinical severity score system in dogs with degenerative mitral valve disease. *J Vet Intern Med.* 29(2):575–581.
- Lord PF, Hansson K, Carnabuci C, Kwart C, Häggström J. 2011. Radiographic heart size and its rate of increase as tests for onset of congestive heart failure in Cavalier King Charles Spaniels with mitral valve regurgitation. *J Vet Intern Med.* 25(6):1312–1319.
- Malik M, Bigger JT, Camm AJ, Kleiger RE, Malliani A, Moss AJ, Schwartz PJ. 1996. Heart rate variability. Standards of measurement, physiological interpretation, and clinical use. Task Force of the European Society of Cardiology and the North American Society of Pacing and Electrophysiology. *Eur Heart J.* 17(3):354–381.
- Moise NS, Brewer FC, Flanders WH, Kornreich BG, Otani NF. 2021. Insights into sinus arrhythmia of the dog: acetylcholine perfusion of canine right atrium results in beat-to-beat patterns that mimic sinus arrhythmia supporting exit block in the sinoatrial conduction pathways. *Vet J.* 272:105651.
- Moise NS, Flanders WH, Pariaut R. 2019. Beat-to-beat patterning of sinus rhythm reveals non-linear rhythm in the dog compared to the human. *Front Physiol.* 10:1548.
- Moise NS, Gladuli A, Hemsley SA, Otani NF. 2010. Zone of avoidance: RR interval distribution in tachograms, histograms, and Poincaré plots of a Boxer dog. *J Vet Cardiol.* 12(3):191–196.
- Oliveira MS, Muzzi RAL, Araújo RB, Muzzi LAL, Ferreira DF, Silva EF. 2014. Heart rate variability and arrhythmias evaluated with Holter in dogs with degenerative mitral valve disease. *Arq Bras Med Vet Zootec.* 66(2):425–432.
- Ootaki C, Manzo A, Kamohara K, Popović ZB, Fukamachi K, Ootaki Y. 2008. Heart rate variability in a progressive heart failure model with rapid ventricular pacing. *Heart Surg Forum.* 11(5):E295–E299.
- Pirintr P, Saengklub N, Limprasutr V, Sawangkoon S, Kijtawornrat A. 2017. Sildenafil improves heart rate variability in dogs with asymptomatic myxomatous mitral valve degeneration. *J Vet Med Sci.* 79(9):1480–1488.
- Rasmussen CE, Vesterholm S, Ludvigsen TP, Häggström J, Pedersen HD, Moesgaard SG, Olsen LH. 2011. Holter monitoring in clinically healthy Cavalier King Charles Spaniels, Wire-haired Dachshunds, and Cairn Terriers. *J Vet Intern Med.* 25(3):460–468.
- Reinero C, Visser LC, Kellihan HB, Masseau I, Rozanski E, Clercx C, Williams K, Abbott J, Borgarelli M, Scansen BA, et al. 2020. ACVIM consensus statement guidelines for the diagnosis, classification, treatment, and monitoring of pulmonary hypertension in dogs. *J Vet Intern Med.* 34(2):549–573.
- Rishniw M, Brown D. 2022. The ACVIM consensus statement definition of left ventricular enlargement in myxomatous mitral valve disease does not always represent left ventricular enlargement. *J Vet Cardiol.* 42:92–102.
- Romito G, Guglielmini C, Poser H, Baron Toaldo M. 2021. Lorenz plot analysis in dogs with sinus rhythm and tachyarrhythmias. *Animals (Basel).* 11(6):1645.
- Shaffer F, Ginsberg JP. 2017. An overview of heart rate variability metrics and norms. *Front Public Health.* 5:1–17.
- Shaffer F, McCraty R, Zerr CL. 2014. A healthy heart is not a metronome: an integrative review of the heart's anatomy and heart rate variability. *Front Psychol.* 5:1–19.
- Thomas WP, Gaber CE, Jacobs GJ, Kaplan PM, Lombard CW, Moise NS, Moses BL. 1993. Recommendations for standards in transthoracic two-dimensional echocardiography in the dog and cat. Echocardiography Committee of the Specialty of Cardiology, American College of Veterinary Internal Medicine. *J Vet Intern Med.* 7(4):247–252.
- Vezzosi T, Domenech O, Costa G, Marchesotti F, Venco L, Zini E, Del Palacio MJF, Tognetti R. 2018. Echocardiographic evaluation of the right ventricular dimension and systolic function in dogs with pulmonary hypertension. *J Vet Intern Med.* 32(5):1541–1548.
- Zhou S-X, Lei J, Fang C, Zhang Y-L, Wang J-F. 2009. Ventricular electrophysiology in congestive heart failure and its correlation with heart rate variability and baroreflex sensitivity: a canine model study. *Europace.* 11(2):245–251.